MPI-PhT/2003-34
July 2, 2003
gr-qc/0307029

Non-Abelian gravitating solitons with negative cosmological constant

Peter Breitenlohner, Dieter Maison

Max-Planck-Institut für Physik
— Werner Heisenberg Institut —
Föhringer Ring 6
D-80805 Munich, Germany

and
George Lavrelashvili

Department of Theoretical Physics
A.Razmadze Mathematical Institute
GE-0193 Tbilisi, Georgia

Abstract

Static, spherically symmetric solutions with regular origin are investigated of the Einstein-Yang-Mills theory with a negative cosmological constant Λ. A combination of numerical and analytical methods leads to a clear picture of the 'moduli space' of the solutions. Some issues discussed in the existing literature on the subject are reconsidered and clarified. In particular the stability of the asymptotically AdS solutions is studied. Like for the Bartnik-McKinnon (BK) solutions obtained for $\Lambda = 0$ there are two different types of instabilities – 'topological' and 'gravitational'. Regions with any number of these instabilities are identified in the moduli space. While for BK solutions there is always a non-vanishing equal number of instabilities of both types, this degeneracy is lifted and there exist stable solutions, genuine sphalerons with exactly one unstable mode and so on. The boundaries of these regions are determined.

1 Introduction

The last decade has witnessed an intensive study of soliton and black hole solutions of the Einstein-Yang-Mills (EYM) theory leading to many unexpected re-

sults (see [1] for a review). In particular it turned out that the strong uniqueness theorems for such solutions valid for gravitating Abelian gauge fields (Einstein-Maxwell theory) cease to hold in the non-Abelian case. Also the stability properties of spherically symmetric solutions change, partly due to the breakdown of the Birkhoff theorem in the non-Abelian theory.

Among the many possible extensions of the EYM system studied in the literature the simplest one is obtained by adding a cosmological constant Λ [2, 3]. As to be expected this changes the global behavior of the regular solutions in a characteristic way from asymptotically Minkowskian to that of deSitter (dS) resp. Anti-deSitter space (AdS) depending on the sign of Λ. This change is also accompanied by a change of the moduli space of globally regular ('soliton') and black hole solutions. While for a given $\Lambda \geq 0$ the generic solution is singular and there is only a discrete set of soliton solutions (characterized by the node-number of the YM potential W) there are two types of generic solutions for $\Lambda < 0$, the singular ones and asymptotically AdS solutions with continuously varying values W_∞ of W at $r = \infty$. This change of the topology of the moduli space going from negative to positive values of Λ leads to, what was called a 'fractal' structure in [4].

A further important difference between the dS and AdS case concerns the stability properties of the solutions. While it was found that all solutions with $\Lambda > 0$ are still unstable like the Bartnik-McKinnon (BK) solutions [5] obtained for $\Lambda = 0$ there exist stable solutions with AdS asymptotics for negative cosmological constant [4, 6]. In fact, there seems to be general agreement in the literature [4, 6, 7, 8, 9] that all solutions with a nodeless YM potential W are stable. For soliton solutions the question was studied numerically in [4] and stability was found for certain solutions with no or one node. An analytical proof was given in [6] for black holes with $W_h > 1/\sqrt{3}$ and in [10, 11] for nodeless solitons, however in both cases assuming $\Lambda \ll 0$. How the authors of [4, 6] arrive at their general statement that all nodeless solutions are stable remains unclear and in fact we shall present convincing arguments that it is wrong. In addition we give a short discussion of the concept of stability employed in the above considerations.

As in the case $\Lambda \geq 0$ there are two different types of spherically symmetric unstable modes, those of 'topological' type (odd parity) and 'gravitational' ones (even parity). While for the BK solutions there is always an equal number of unstable modes of both types directly given by the number of nodes of the solution [12] this is not true for $\Lambda \leq 0$.

Our investigation of the stability properties of the soliton solutions is based on a general study of the moduli space of the solutions as a function of Λ. In particular we find two discrete sets of lines in the (Λ, b) plane, (where b parametrizes the solutions with a regular origin), separating regions with a different number of unstable modes. First there are the lines with vanishing W_∞ for solutions with n nodes. Crossing these lines the number of odd parity unstable modes changes by one [7, 13]. Furthermore there is a discrete set of lines of zero-modes in the (Λ, b) plane separating regions with a different number of even parity unstable modes. Besides the region in the moduli space without unstable modes there are regions with exactly one unstable mode, the

condition for a genuine sphaleron like the traditional one in flat space [14]. This may have some interesting consequences for the application.

Combining numerical with analytical tools we give a detailed description of the boundary between the domain of asymptotically AdS and the singular solutions yielding a simple explanation of the 'fractal' structure observed in [4]. In particular, based on earlier work [15] on the BK solutions we will derive a scaling law for the small Λ part of the boundary between these two domains.

For reasons of simplicity we have restricted ourselves to electrically neutral soliton solutions, but the generalization to charged solutions and black holes should be straightforward.

2 Field Equations

The action of EYM theory with the cosmological constant Λ has the form

$$S_{\mathrm{EYM}_\Lambda} = \frac{1}{4\pi}\int\Big(-\frac{1}{4G}(R+2\Lambda) - \frac{1}{4g^2}F^a_{\mu\nu}F^{a\mu\nu}\Big)\sqrt{-g}d^4x\ , \tag{1}$$

where G is Newton's constant and g is the gauge coupling. In what follows we put $G = g = 1$ choosing suitable units.

We will be interested in spherically symmetric solutions with regular origin. For a spherically symmetric space-time the line element decomposes into

$$ds^2 = ds_2^2 - r^2 d\Omega^2\ , \tag{2}$$

where ds_2^2 is the metric on the 2-d orbit space factorizing out the action of the rotation group and $d\Omega^2$ the invariant line element of S^2. The 2-d metric can always be brought to the diagonal form

$$ds_2^2 = \Big(e^{2\nu}dt^2 - e^{2\lambda}dR^2\Big)\ , \tag{3}$$

where t is a time-like coordinate. Here we are only considering time-independent solutions and we naturally choose t to be the Killing time. This means that we can perform a further dimensional reduction to a 1-d theory. Then the metric functions ν, λ and r depend only on the radial coordinate R. The latter can be chosen arbitrarily exhibiting λ as a gauge degree of freedom.

For the *SU(2)* Yang-Mills field W^a_μ we use the standard minimal spherically symmetric (purely 'magnetic') ansatz

$$W^a_\mu T_a dx^\mu = W(R)(T_1 d\theta + T_2\sin\theta d\varphi) + T_3\cos\theta d\varphi\ , \tag{4}$$

where T_a denote the generators of *SU(2)*. The reduced EYM action including a negative cosmological constant Λ can be expressed as

$$\begin{aligned} S = -\int dR\, e^{(\nu+\lambda)}\Big[\frac{1}{2}\Big(1 + e^{-2\lambda}((r')^2 + \nu'(r^2)')\Big) \\ -e^{-2\lambda}r^2\frac{(W')^2}{r^2} - \frac{(1-W^2)^2}{2r^2} + \frac{|\Lambda|r^2}{2}\Big]\ . \end{aligned} \tag{5}$$

Introducing

$$N \equiv e^{-\lambda} r' \,, \quad \kappa \equiv r e^{-\lambda} \nu' + N \,, \quad U \equiv e^{-\lambda} W' \,, \tag{6}$$

we write the corresponding Euler-Lagrange equations in first order form

$$r e^{-\lambda} N' = \Big(\kappa - N\Big) N - 2U^2 \,, \tag{7a}$$

$$r e^{-\lambda} \kappa' = 1 + 2|\Lambda| r^2 + 2U^2 - \kappa^2 \,, \tag{7b}$$

$$r e^{-\lambda} U' = \frac{W(W^2-1)}{r} + \Big(N - \kappa\Big) U \,, \tag{7c}$$

$$2\kappa N - N^2 = 2U^2 + 1 - \frac{(1-W^2)^2}{r^2} + |\Lambda| r^2 \,. \tag{7d}$$

The last of these equations is the only remaining diffeomorphism constraint.

We still have to fix the gauge, i.e. choose a radial coordinate. A simple choice is to use the geometrical radius r for R (Schwarzschild coords.), yielding $e^{-\lambda} = N$. Putting $\mu \equiv N^2$, $A \equiv e^{\nu}/N$, and $\Lambda = 0$, Eqs. (7) become equal to Eqs. (6) in [15]. This coordinate choice has the disadvantage that the equations become singular at stationary points of r. This problem is avoided using the gauge $e^{\lambda} = r$ introduced in [15], which will also be used here. In order to stress the dynamical systems character of Eqs. (6,7) we denote the corresponding radial coordinate by τ and derivatives by a dot. We thus get

$$\dot{r} = rN \,, \tag{8a}$$

$$\dot{\nu} = \kappa - N \,, \tag{8b}$$

$$\dot{W} = rU \,, \tag{8c}$$

$$\dot{N} = (\kappa - N) N - 2U^2 \,, \tag{8d}$$

$$\dot{\kappa} = 1 + 2|\Lambda| r^2 + 2U^2 - \kappa^2 \,, \tag{8e}$$

$$\dot{U} = \frac{W(W^2-1)}{r} + (N - \kappa) U \,, \tag{8f}$$

Using the constraint Eq. (7d) the equation for N can also be written as

$$\dot{N} = \frac{1}{2}\Big(1 + |\Lambda| r^2 - \frac{(W^2-1)^2}{r^2})\Big) - \frac{1}{2} N^2 - U^2 \,. \tag{9}$$

For $\Lambda = 0$ these equations coincide with the Eqs. (49,50) of [15]. An important quantity is the 'mass function' $m = r(1 + |\Lambda| r^2/3 - N^2)/2$ obeying the equation

$$\dot{m} = \left(U^2 + \frac{(W^2-1)^2}{2r^2}\right) rN \,. \tag{10}$$

The value m_∞ of m at $r = \infty$ is the AdS mass of the solution. Due to the presence of the cosmological constant the vacuum solution obtained for $W^2 = 1$ is no longer Minkowski space but Anti-deSitter (AdS) space

$$ds^2 = \mu dt^2 - \frac{dr}{\mu} - r^2 d\Omega^2 \,, \tag{11}$$

with

$$\mu(r) = 1 + \frac{|\Lambda| r^2}{3} \,, \tag{12}$$

while the counterpart of the Schwarzschild solution for $\Lambda < 0$ is the Schwarzschild-AdS solution obtained for

$$\mu(r) = 1 - \frac{2M}{r} + \frac{|\Lambda| r^2}{3} \,, \tag{13}$$

describing a black hole with AdS asymptotics for $M > 0$.

Likewise there is the Reissner-Nordstrøm-AdS (RN) solution for $W = 0$ and

$$\mu(r) = 1 - \frac{2M}{r} + \frac{1}{r^2} + \frac{|\Lambda| r^2}{3} \,, \tag{14}$$

carrying an Abelian magnetic charge. The function μ has either two simple zeros, a double zero or no zero at all for positive r. The double zero occurs at $r_0^2 = (\sqrt{1 + 4|\Lambda|} - 1)/2|\Lambda|$ for a certain value $M_0(|\Lambda|)$. As long as μ has zeros the solution describes a charged black hole with AdS asymptotics. The zero of μ at the smaller value of r corresponds to the Cauchy horizon of the Reissner-Nordstrøm black hole. A double zero of μ is the position of an extremal horizon. Solutions without zero have a naked singularity at the origin.

3 Global behavior

We want to study the global behavior of solutions with a regular origin. As in the case without cosmological constant the field equations (8) are singular for $r = 0$, but using the methods of [15] it is straightforward to show that there is a 2-parameter family of regular solutions with the behavior

$$W(r) = 1 - br^2 + \frac{1}{10} b(3b - 8b^2 + 2|\Lambda|) r^4 + O(r^6) \,, \tag{15a}$$

$$\mu(r) = 1 - (4b^2 - \frac{|\Lambda|}{3}) r^2 + \frac{16}{15} b^2 (3b + |\Lambda|) r^4 + O(r^6) \,, \tag{15b}$$

$$A(r) = A_0 \Big(1 + 4b^2 r^2 - \frac{4b^2}{5} (3b - 18b^2 + 2|\Lambda|) r^4 + O(r^6) \Big) \,, \tag{15c}$$

where b and A_0 are free parameters. A trivial rescaling of the time coordinate t allows to put $A_0 = 1$ and we will assume this condition henceforth for solutions with a regular origin.

We may start with a solution with this behavior at $r = 0$ and integrate the field equations (8) for increasing τ. This way we can extend the solution until we hit a singular point for some finite value τ_s or otherwise to arbitrarily large values of τ. As long as $N(\tau)$ is positive $r(\tau)$ will grow monotonously. However, $N(\tau)$ may have a zero for some value τ_0. If the function A would stay bounded at τ_0 this would lead to a zero of the metric coefficient $e^{2\nu}$ implying a (cosmological) horizon. However, it is easy to see from Eq. (8e) that this is impossible, because $\kappa \geq 1$. Thus the function μ cannot become negative as is e.g. claimed in [4]. In fact it is only the function N that becomes negative

and consequently the function $r(\tau)$ has a maximum and decreases for larger τ. It follows from Eq. (8d) that N, once negative, cannot become positive again. As in the case without cosmological constant one can show that N tends to $-\infty$ for some finite value τ_s and r runs back to zero. There the solution becomes singular in complete analogy to the case $\Lambda = 0$ [15], since the terms proportional to Λ may be neglected for $r \to 0$. One finds a Reissner-Nordstrøm type singularity of the metric [17]

$$W(r) = W_0 + \frac{W_0}{2(1-W_0^2)} r^2 + W_3 r^3 + O(r^4) \,, \tag{16a}$$

$$\mu(r) = \frac{(W_0^2-1)^2}{r^2} - 2\frac{M_0}{r} + O(1) \,, \tag{16b}$$

$$A(r) = A_0 + O(r^2) \,. \tag{16c}$$

with the arbitrary parameters W_0, W_3, M_0 and A_0. Topologically the 2-spheres of fixed r of these solutions foliate a 3-sphere with a singularity at its second 'origin', suggesting to call them 'Singular Compact' solutions' (SC). From the number of parameters it follows that this is a 'generic' class of solutions.

The situation where $N(\tau)$ stays positive is a bit more involved and we will have to distinguish three cases. Since $r(\tau)$ is monotonously growing it will either have a finite limit or it will tend to infinity. In the first case the situation is practically the same as without cosmological constant. Following the arguments given in [15] one concludes that the solution exists for all τ and tends for $\tau \to \infty$ to the fixed point corresponding to the degenerate horizon of the extremal RN black hole with $(r, W, U, N, \kappa) = (r_0, 0, 0, 0, \kappa_0)$ where $r_0^2 = (\sqrt{1+4|\Lambda|}-1)/2|\Lambda|$ and $\kappa_0^2 = \sqrt{1+4|\Lambda|}$. Linearizing the Eqs. (8) around this point exhibits the hyperbolic character of the fixed point with eigenvalues κ_0, -2, $-\kappa_0(1 \pm \gamma)/2$ where $\gamma^2 = 1 - 4/\sqrt{1+4|\Lambda|}$. As long as $|\Lambda| < 15/4$ there are two complex conjugate eigenvalues leading to damped oscillating eigenfunctions, while for $|\Lambda| \geq 15/4$ these eigenvalues are real and negative. As in the $\Lambda = 0$ case the space-time splits into two separate parts. The exterior part is the exterior (to the degenerate horizon) of the extremal RN-AdS black hole and is geodesically incomplete, while the interior part containing the origin is a geodesically complete manifold with the topology of AdS and not a space with a boundary as claimed in [7].

In the second case $r \to \infty$ there remain two possibilities; either the solution is asymptotically AdS with finite mass $M = \lim_{r\to\infty} m(r)$ or it is a new singular solution, with the mass function $m(r)$ diverging as r^3. The AdS type solutions have the asymptotic behavior (we use again Schwarzschild coordinates)

$$W(r) = W_\infty + \frac{c}{r} + \frac{3W_\infty({W_\infty}^2-1)}{2|\Lambda|}\frac{1}{r^2} + O\left(\frac{1}{r^3}\right) \,, \tag{17a}$$

$$\mu(r) = 1 - \frac{2M}{r} + \frac{|\Lambda|}{3} r^2 + (({W_\infty}^2-1)^2 + \frac{2}{3}|\Lambda| c^2)\frac{1}{r^2} + O\left(\frac{1}{r^3}\right) \,, \tag{17b}$$

$$A(r) = A_\infty\left(1 - \frac{c^2}{2r^4} + O\left(\frac{1}{r^5}\right)\right) \,, \tag{17c}$$

with the arbitrary parameters W_∞, c, M, and A_∞. Like the 'SC' solutions this is a generic class of solutions. From the linear growth of $N = \sqrt{\mu}$ with r it follows that τ remains finite for $r \to \infty$.

Apart from this regular AdS behavior at infinity there is a singular class of solutions (called SAdS) with W, U, N, and κ growing linearly with r. For their description we introduce new variables

$$\bar{W} = \frac{W}{r} \,, \quad \bar{\mu} = \frac{\mu}{r^2} \,, \quad \text{and} \quad V = \bar{\mu} W' \,. \tag{18}$$

In terms of these variables the field equations become

$$r\bar{W}' = \frac{V}{\bar{\mu}} - \bar{W} \,, \tag{19a}$$

$$rV' = \bar{W}(\bar{W}^2 - \frac{1}{r^2}) - 2V - \frac{2V^3}{\bar{\mu}^2} \,, \tag{19b}$$

$$r\bar{\mu}' = -3\bar{\mu} - \frac{2V^2}{\bar{\mu}} - (\bar{W}^2 - \frac{1}{r^2})^2 + |\Lambda| + \frac{1}{r^2} \,. \tag{19c}$$

The singular solution corresponds to a hyperbolic fixed point of these equations for $r \to \infty$ with finite values $\bar{W}_0, V_0, \bar{\mu}_0$ determined by the vanishing of the r.h.s. These values can be expressed in terms of $x \equiv \bar{W}_0^2$ obeying the cubic equation

$$2x^3 + 4x^2 + 3x - 2|\Lambda|(1+x) = 0 \,, \tag{20}$$

which has always one positive root. The values V_0 and $\bar{\mu}_0$ at the fixed point can be expressed in terms of x as $V_0 = \frac{1}{2}x^{3/2}/(1+x)$ and $\bar{\mu}_0 = \frac{1}{2}x/(1+x)$. Introducing $w = \bar{W} - \sqrt{x}$, $v = V - V_0$, and $\chi = \bar{\mu} - \bar{\mu}_0$ and linearizing Eqs. (19) in these shifted variables we obtain

$$rw' = -w + \frac{2(1+x)}{x} v - \frac{2(1+x)}{\sqrt{x}} \chi \,, \tag{21a}$$

$$rv' = 3w - 2(1+3x)v + 4x\sqrt{x}\chi \,, \tag{21b}$$

$$r\chi' = -4x\sqrt{x}w - 4\sqrt{x}v + (2x-3)\chi \,. \tag{21c}$$

Studying the characteristic equation of this linear system one finds that its eigenvalues are always real for $x > 0$. Since for $x \to 0$ the eigenvalues become $1, -3, -4$ and the determinant $16x^3 + 40x^2 + 32x + 12$ is positive for $x > 0$ there is exactly one unstable mode for any $|\Lambda| > 0$.

Our numerical analysis shows that any solution with regular origin belongs to one of the types described above and it would be desirable to prove this analytically. All the considered solutions have some well-defined asymptotics and thus there is no indication of any chaotic behavior.

4 Moduli space topology

Next we want to describe the moduli space of the solutions with regular origin as obtained from a thorough numerical analysis supported by analytical arguments. Our numerical results are obtained using a shooting technique

starting from $r = 0$ (not from e.g. $r = 10^{-3}$) combined with integral equations if necessary as described in [16]. For given Λ the solutions depend only on the parameter b. In contrast to the case without cosmological constant there are now two different types of 'generic' solutions, the 'Singular Compact' ones running back to $r = 0$ already present for $\Lambda = 0$ and those with AdS asymptotics. Therefore we expect certain open sets in the (Λ, b) plane corresponding to these two types. Fig. 1 gives a schematic description of these open sets. The domain called 'AdS' corresponds to the AdS type solutions. It has a rather complicated boundary, consisting of the curves 'RN' and 'SAdS'. The latter consists of the lower boundary and infinitely many arcs connecting the points $(\Lambda, b) = (0, b_n)$, where the b_n's are those of the n^{th} BK solution.[1] The set 'AdS' may be further subdivided according to the number of nodes of W as indicated in Fig. 1.

The complement of the closure of 'AdS' corresponds to the 'SC' solutions. It consists of the disconnected pieces 'S_n' ($n = 0, 1 \ldots$), containing solutions with n zeros of W and $|W_0| > 1$. Furthermore there is the set S_∞ containing solutions with any number of zeros but with $|W_0| < 1$. These sets are in close correspondence with those introduced in [15]. Since the intervals between the b_n's on the Λ-axis belong to the sets 'S_n' and the latter are open, they extend into the region $\Lambda \neq 0$, but as will be explained later, their boundaries become numerically very quickly indistinguishable from the Λ-axis for larger values of n. Varying the parameter b for fixed Λ closer and closer to the axis one intersects more and more of the sets 'S_n' alternating with intervals in 'AdS'. This explains the 'fractal' structure close to the Λ-axis observed in [4].

The left and lower boundary ('SAdS') of 'AdS' corresponds to the singular solutions with unbounded $W(r)$. Hence W_∞ in 'AdS' resp. W_0 in 'S_n' becomes arbitrarily large approaching these boundaries.

The upper boundary curve 'RN' of 'AdS' corresponds to solutions running into the RN fixed point described in the previous section. It starts at the value $b_\infty \approx 0.7642$ of [15] yielding the limiting solution of the BK family for $\Lambda = 0$. For $|\Lambda| < 15/4$ the corresponding solutions have infinitely many zeros and hence the neighborhood of this piece of the boundary contains solutions with arbitrarily many zeros.

Figs. 2 and 3 show the same moduli space as Fig. 1, but this time with actual numerical data. The dotted curves describe solutions with constant values W_∞ resp. W_0. All the W_∞ curves emanate from the BK values $(0, b_n)$ on the Λ-axis. Crossing the dashed-dotted lines $W_\infty = 0$ the number of zeros of W changes by one. The lowest of these lines separates solutions without zero from those with exactly one. It bifurcates with the 'RN' boundary curve at the point P_0 with $|\Lambda| \approx 5.0646$, while all the other zero lines bifurcate with 'RN' at P_∞ with $|\Lambda| = 15/4$.

It is easy to understand that the region where $b \gg \sqrt{|\Lambda|}$ belongs to 'S_∞'. There the Λ term can be neglected and the situation is the same as for $\Lambda = 0$. The same holds for $b \ll -\sqrt{|\Lambda|}$ corresponding to the region $b \ll 0$ for $\Lambda = 0$. In the next section we shall derive more detailed properties of the boundary curves.

[1] We include the trivial solution $W \equiv 1$ obtained for $b_0 = 0$.

5 Boundary Curves

The boundary curves are given by non-generic solutions corresponding to fixed points with one unstable mode. Hence they have to be determined by fine-tuning one of the parameters b or Λ.

In order to determine the 'RN' curve one takes solutions running into the RN fixed point. As mentioned in section 3 such solutions are oscillating as long as $|\Lambda| < 15/4$. For $|\Lambda| > 15/4$ these solutions can have only a finite number of zeros. In fact, our numerical analysis shows that they have exactly one zero for $15/4 < |\Lambda| < L_1$ with $L_1 \approx 5.0646$ (the point P_0 of Figs. 1 and 2) and no zeros for larger values of $|\Lambda|$. Therefore all the curves $W_\infty = 0$ in 'AdS' with more than one zero merge with 'RN' exactly at $|\Lambda| = 15/4$ (the point P_∞), while the lowest curve with one zero merges with 'RN' at P_0. The curves for nodeless solutions with $0 < W_\infty < 1$ run out to $|\Lambda| = \infty$ eventually approaching the boundary 'RN'.

Next we shall consider the asymptotic behavior of the boundary for large values of $|\Lambda|$. As a first step we rescale $r \to \bar{r} \equiv |\Lambda|^{1/2} r$ in order to remove the explicit Λ dependence from the field equations. To retain the expansions Eq. (15b,c) at $r = 0$ we have to compensate this by a corresponding rescaling of $b \to \bar{b} \equiv |\Lambda|^{-1/2} b$. In fact, the expansion Eq. (15a) for W even requires to put $\bar{b} = 1/2$. Thus asymptotically the boundary of 'AdS' becomes the parabola $|\Lambda| = 4b^2$. Fig. 4 shows the remarkably perfect fit of the boundary with the (empirically adapted) parabola $|\Lambda| = 4b^2 - 3b - 0.1$ even for small values of $|\Lambda|$.

The asymptotic form of the solution on 'RN' can also be obtained rather simply. Introducing $\bar{W} \equiv (W-1)/r$ we find

$$\bar{W} = -\bar{r}/2 + O(|\Lambda|^{-1/2}) \,, \tag{22a}$$

$$U = -\bar{r}N + O(|\Lambda|^{-1/2}) \,. \tag{22b}$$

Neglecting non-leading terms the Eq. (9) for N becomes

$$\dot{N} = \bar{r}N\frac{dN}{d\bar{r}} = \frac{1}{2}(1 - N^2 - 2U^2 - 4\bar{W}^2 + \bar{r}^2) = \frac{1}{2}(1 - N^2 - 2\bar{r}^2 N^2) \,. \tag{23}$$

This linear equation for $N^2 = \mu$ can be solved imposing the boundary condition $\mu(0) = 1$ with the simple result

$$\mu = \frac{\mathrm{e}^{-\bar{r}^2}}{\bar{r}} \int_0^{\bar{r}} \mathrm{e}^{r'^2} dr' \,. \tag{24}$$

For $\bar{r} \to \infty$ the solution behaves as $N = \bar{r}^{-1}/\sqrt{2} + O(\bar{r}^{-2})$ and $U = -1/\sqrt{2} + O(\bar{r}^{-2})$.

It seems to be much more difficult to obtain an asymptotic form of the SAdS solutions for $|\Lambda| \to \infty$ as compared to the solutions running into the RN fixed point.

The left boundary of 'AdS' with its infinitely many arcs looks at first sight rather complicated. However, making use of the results of [15] we shall derive a simple scaling law for the asymptotic form of these arcs for large n.[2] The

[2] A similar argument was used in [8] to derive a scaling law for the ADM mass of the solutions.

basic idea is to relate the neighborhood of the points $(0, b_n)$ to that of the point $(0, b_0 = 0)$. As a first step we consider the solutions with $|\Lambda| \ll 1$ and $|b| \ll 1$.

A suitable rescaling in this case is again $\bar{r} \equiv \sqrt{|\Lambda|} r$. Putting $\bar{U} \equiv |\Lambda|^{-1/2} U$ and keeping only leading terms in $|\Lambda|$ we obtain from Eqs. (8)

$$\dot{\bar{r}} = \bar{r} N \ , \tag{25a}$$

$$\dot{N} = (\kappa - N) N \ , \tag{25b}$$

$$\dot{\kappa} = 1 + 2\bar{r}^2 - \kappa^2 \ , \tag{25c}$$

$$\dot{W} = \bar{r} \bar{U} \ , \tag{25d}$$

$$\dot{\bar{U}} = W(W^2 - 1)/\bar{r} + (N - \kappa)\bar{U} \ , \tag{25e}$$

together with the constraint

$$2\kappa N - N^2 = 1 + \bar{r}^2 \ . \tag{26}$$

Since the equations for N and κ are free of matter terms we obtain the AdS metric. The remaining Eqs. (25d,e) for W and $\bar{U}$ are just those for the YM field in the AdS background with $|\Lambda| = 1$. Clearly we have to rescale also $b \equiv |\Lambda| \bar{b}$ to obtain the expansion $W = 1 - \bar{b}\bar{r}^2 + O(\bar{r}^4)$ at the origin.

Numerically one finds a finite interval $\bar{b}_0 < \bar{b} < \bar{b}_1$ with $\bar{b}_0 \approx -0.294582$ and $\bar{b}_1 \approx 2.970497$ for which W stays bounded. Outside this interval W diverges for finite $\bar{r}$. There is an exact solution [18] $W(\bar{r}) = (1 + \bar{r}^2/3)^{-1/2}$ corresponding to $\bar{b} = 1/6$, which separates solutions with and without zero, solutions for $\bar{b} \leq 1/6$ having no zero, while solutions with $\bar{b} > 1/6$ having exactly one.

Next we analyze the boundary in the neighborhood of the BK points $(\Lambda, b) = (0, b_n)$. In [15] it was argued that for $b \approx b_n$ there is some $r_n \approx r_0 e^{\frac{n\pi}{\sqrt{3}}}$ such that for $r \approx r_n$ the solution can be parametrized in the form

$$N(r) = 1 - \frac{M_n(b, r)}{r} \ , \tag{27a}$$

$$W(r) = (-1)^n \Big(1 - b_n^{(\infty)}(r, b) r^2 - \frac{c_n(r, b)}{r} \Big) \ , \tag{27b}$$

with slowly varying functions M_n, $b_n^{(\infty)}$, and c_n. While the coefficients of the convergent modes $M_n(b, r)$ and $c_n(b_n, r)$ have non-zero limits for $r \to \infty$ that of the divergent mode $b_n^{(\infty)}(b_n, r)$ vanishes in this limit. However, assuming transversality its derivative $\partial b_n^{(\infty)}(b_n, r)/\partial b$ has a non-zero limit $b_n^{\infty,1}$ and thus $b_n^{(\infty)} \approx b_n^{\infty,1}(b - b_n)$. Taking $r \gg r_n$ and $b - b_n \ll 1$ we can neglect the terms with M_n and c_n still keeping $b_n^{(\infty)} r^2 \ll 1$. This implies the relations $N \approx 1$ and $U/2 \approx (W \pm 1)/r$ characterizing the stable manifold of the singular point $r = 0$, i.e. valid near $r = 0$ for solutions with a regular origin. Thus we succeeded to relate solutions with $b \approx b_n$ to solutions with $b \approx 0$. All this remains true for non-zero $|\Lambda| \ll 1$ and we can repeat the arguments from above for small Λ and b. Rescaling again $r \to \bar{r} = |\Lambda|^{1/2} r$ we will find the same behavior of the solution with $b \approx b_n$ for $r \gg r_n$ as with $b \approx 0$ for $\bar{r} > 0$ if $\bar{b} = b_n^{(\infty)} |\Lambda|^{-1} \approx b_n^{\infty,1}(b - b_n)|\Lambda|^{-1}$. Arguments analogous to the ones used in [15] to derive scaling laws for the parameters of BK solutions with large n show

that $b_n^{\infty,1}$ scales like $r_n^{-2} \approx \text{const.} \cdot e^{-\frac{2n\pi}{\sqrt{3}}}$. Therefore we expect to find the same linear relation $b = \bar{b}_{0,1}|\Lambda|$ valid for the boundary curves near $(\Lambda, b) = (0, 0)$ also near the points $(0, b_n)$, if we rescale Λ by the factor $e^{-\frac{2n\pi}{\sqrt{3}}} \sim (b_\infty - b)^2$. Fig. 5 shows this scaling law is in fact well satisfied already from $n = 3$ on and even holds not only for the whole arcs joining subsequent b_ns, but also the neighboring curves of constant W_∞ resp. suitably rescaled W_0.

The scaling argument for the singular solutions parametrized by W_0 has to be different from that for the AdS ones. The singular solutions start from a regular origin $r = 0$, have a maximum of r ('equator') at some point $r = r_e$ and then run back to $r = 0$, where $N \to -\infty$. In [15] an asymptotic formula for r_e, W_e, and U_e for small values of b was derived for the case $\Lambda = 0$

$$r_e \approx \bar{r}|b|^{-\frac{1}{2}} , \qquad |W_e| \approx 2^{-\frac{1}{6}} 3^{\frac{1}{3}} r_e^{\frac{2}{3}} , \qquad |U_e| \approx \frac{W_e^2}{\sqrt{2} r_e} , \tag{28}$$

where $\bar{r} \approx 5.317$ for $b > 0$ and $\bar{r} \approx 1.746$ for $b < 0$. Observe that W_e grows as $|b|^{-1/3}$ for $b \to 0$. The derivation of these formulae is based on two steps. First the equation for W is integrated on a flat background, leading to a divergence of $|W| \approx 1/(\tau_\infty - \tau)$ for some finite value τ_∞ and a corresponding finite value $r_\infty = \bar{r}|b|^{-1/2}$. The scaling with $|b|^{-1/2}$ is a consequence of the scale invariance of the flat YM equation. The two values of $\bar{r}$ for the two sign choices of b are determined by a numerical integration of the flat YM equation. Using this diverging solution for W, the equation for N is then integrated from $N = 1$ to $N = 0$, the equator, yielding finite values $\tau_e < \tau_\infty$, W_e, U_e, and r_e. Since this change of N happens on a τ interval whose length tends to zero for $b \to 0$, we get $r_e \approx r_\infty$. This derivation remains essentially valid taking into account the cosmological term, but there are two modifications. Firstly, the function W is now considered in the AdS background. This step yields functions $\bar{r}(\bar{b})$ (with $\bar{b} = b/|\Lambda|$) for $b > 0$ resp. $b < 0$, replacing the two values of $\bar{r}$ from the flat case (compare Fig. 6 for a numerical determination). Secondly, the function N has now to run between the AdS value $\sqrt{1 + |\Lambda| r_\infty^2/3}$ and the equator $N = 0$. Hence we obtain

$$r_e \approx \bar{r}(\frac{b}{|\Lambda|})|b|^{-\frac{1}{2}} , \quad |W_e| \approx 2^{-\frac{1}{6}} 3^{\frac{1}{3}} r_e^{\frac{2}{3}} (1 + \frac{|\Lambda| r_e^2}{3})^{\frac{1}{3}} , \quad |U_e| \approx \frac{W_e^2}{\sqrt{2} r_e} , \tag{29}$$

From a systematic point of view it is better not to stop at the equator as was done in [15], but to continue the solution all the way back to $r = 0$ and to characterize it by its value W_0 at $r = 0$. Therefore we decided to plot W_0 instead of W_e (compare Fig. 5). For small values of b one finds $W_0 \gg W_e$, since W_0 scales like $|b|^{-1/2}$ for $b \to 0$ (remember $W_e \sim |b|^{-1/3}$). In order to describe the growth of W between the equator and the singular origin we rescale all the variables W ,U, r, N, κ and also the independent variable τ by $W \to \bar{W}|b|^{-1/2}$ etc. and use approximate equations derived from Eqs. (8) keeping only leading terms for $b \to 0$

$$\dot{\bar{r}} = \bar{r}\bar{N} , \tag{30a}$$

$$\dot{\bar{W}} = \bar{r}\bar{U} , \tag{30b}$$

$$\dot{\bar{N}} = (\bar{\kappa} - \bar{N})\bar{N} - 2\bar{U}^2 \ , \tag{30c}$$

$$\dot{\bar{\kappa}} = 2\bar{U}^2 - \bar{\kappa}^2 \ , \tag{30d}$$

$$\dot{\bar{U}} = \frac{\bar{W}^3}{\bar{r}} + (\bar{N} - \bar{\kappa})\bar{U} \ , \tag{30e}$$

Observe that there is no more dependence on Λ in these equations. In the limit $b \to 0$ the rescaling stretches the finite τ interval to infinite length and the equator becomes a fixed point of the approximate equations. Because of the different scaling at the equator all the rescaled variables $\bar{W}$ etc. vanish at this fixed point like negative powers of τ with fixed coefficients. The only free parameter (apart from the sign of W) is the value r_e of r. Integrating the Eqs. (30) numerically over the infinite τ interval from $r = r_e$ to $r = 0$ we find $|W_0| \approx 1.14871 r_e$. Using Eq. (29) we obtain the simple relation

$$|W_0| = 1.14871 \frac{2^{\frac{1}{4}}}{3^{\frac{1}{2}} \sqrt[4]{1 + \frac{|\Lambda|}{3} r_e^2}} |W_e|^{\frac{3}{2}} \ . \tag{31}$$

The argument about the mapping of the neighborhood of the points $(0, b_n)$ to that of $(0, 0)$ by a suitable scaling works as for the asymptotically AdS solutions with one difference. In contrast to W_∞ the quantity W_0 has to be rescaled, since $W_0 \sim {b_n^{(\infty)}}^{-1/2} \sim e^{\frac{n\pi}{\sqrt{3}}}$. Correspondingly the W_0 curves in Fig.5 refer to W_0 values rescaled by a factor $e^{\frac{\pi}{\sqrt{3}}} \approx 6$ from one S_n domain to the next. Since the relation (31) does not refer to n it should hold equally well in all sectors S_n. Since it is derived for $|W_0| \gg |W_e| \gg 1$ it is easier to test for larger n because of the rescaling. Fig.7 displays how well this relation is satisfied for some selected values of W_0 and n.

6 Stability

While the BK solutions as well as their counterparts for $\Lambda > 0$ studied in [2, 3, 19] are known to be unstable [20, 21] it was observed in [4, 6, 7] that solutions in a certain sub-domain of 'AdS' are stable. Actually, as for BK solutions there are two different kinds of instabilities. There are instabilities of 'topological' type ('odd parity' sector) comparable to those of the flat space sphalerons [22] and 'gravitational' ones ('even parity' sector) [12, 20]. As was shown in [13] for the BK solutions and generalized to solutions with $\Lambda > 0$ in [21], the number of unstable modes of the topological type is equal to the number of zeros of W. Although the same seems to be true empirically in the BK case in the even parity sector there is no general proof (although there is a rather convincing argument [12]). If these rules would be true also for $\Lambda < 0$ one would expect stability in both sectors for solutions in 'AdS' without zero of W, as was claimed in [4]. Although the proof for the odd parity perturbations can be generalized to $\Lambda < 0$ [7, 10], the situation for the even ones is more subtle. In fact, we shall provide numerical evidence that the claim in [4, 6, 7] is wrong and not all the nodeless solutions are stable.

Before entering the detailed discussion of our numerical results, we would like to discuss some more general aspects of the stability issue. Stability is

meant here, as well as in the literature mentioned above, to be stability on the linearized level, i.e. under infinitesimal perturbations. In the present context of a stationary background the perturbations are conveniently decomposed into Fourier modes with respect to the Killing time t and stability means absence of imaginary frequencies, i.e. exponentially growing modes. The linear differential equations for these Fourier modes contain in general some gauge degrees of freedom (independently from the gauge chosen for the background solution), which have to be fixed. Clearly the gauge modes have to be separated out and the physical spectrum should be gauge independent. However, the structure of the resulting linear system may be quite different and favor some particular gauge choices. Apart from that there is a choice of boundary conditions to be made. The latter has two basically different aspects. On the one hand there may be physical conditions for the behavior of the perturbations on the boundary, on the other hand one usually requires self-adjointness of the linear differential operator. The latter is a technical assumption made in order to have an expansion theorem for the general class of perturbations considered. In the case of asymptotically flat solutions one may restrict the consideration to perturbations of compact support, although the eigenmodes themselves will generally not have this property. In this case it is important to have essential self-adjointness of the linear differential operator on the perturbations with compact support in order to fix the spectrum.

Let us now turn to the system under consideration. We shall restrict ourselves to the spherically symmetric perturbations of even parity. It is convenient to use the gauge where the variations are taken at fixed r ('Schwarzschild gauge'), but observe that this does not require the use of Schwarzschild coordinates. In fact, it turns out to be convenient to use a coordinate ρ, for which the 2-d metric is conformally flat putting $dr = A\mu d\rho$. With these conventions the spectral perturbation problem can be reduced as for $\Lambda = 0$ to a single 'Schrödinger equation' [6] for the perturbation δW of W

$$\Big(-\frac{d^2}{d\rho^2} + U(\rho)\Big)\delta W(\rho) = \omega^2 \delta W(\rho)\ , \tag{32}$$

with the potential

$$U(\rho) = A^2\mu\left(\frac{3W^2-1}{r^2} - 4\frac{W'^2}{r^2}\Big(1 - \Lambda r^2 - \frac{(W^2-1)^2}{r^2}\Big) + 8W'\frac{W(W^2-1)}{r^3}\right)\ , \tag{33}$$

where $W' = dW/dr$.

Next we turn to the boundary conditions. In contrast to the asymptotically flat case, where ρ runs from 0 to infinity it runs only over a finite interval $(0, \rho_m]$ in the AdS case. While the potential $U \approx 2/\rho^2$ at $\rho = 0$ is singular it is easily seen to be finite at ρ_m. Correspondingly we are in the 'limit point' case at $\rho = 0$, but in the 'limit cycle' case at ρ_m according to Weyl's classification [23]. This means that the differential symbol does not define an essentially self-adjoint operator, but there is a 1-parameter family of boundary conditions at ρ_m. This is related to the fact, that there are two arbitrary parameters for the background solution at $r = \infty$ (compare Eq. (17)), namely W_∞ and

c. The standard choice in the literature is $\delta W_\infty = 0$ — a choice that looks reasonable, although not much more physical than any condition of the form $\cos\alpha\,\delta W_\infty + \sin\alpha\,\delta c = 0$. Clearly the spectrum of the linear differential operator depends on the boundary condition. Thus the class of perturbations vanishing in a neighborhood of ρ_m do not determine the spectrum uniquely. After all, this is perhaps not too surprising for a space-time, in which time-like geodesics reach $r = \infty$ in a finite coordinate time. Anyhow, in order to be able to compare our results to those in the literature, we make the choice $\delta W_\infty = 0$.

A standard way of analyzing a change of stability is to search for zero modes within a continuous family of solutions [12]. From Fig. 2 it can be seen that all the curves with a fixed value of $W_\infty \neq 0$ with at least one node joining the points $(0, b_n)$ with $(0, b_{n+1})$ have turning points with a maximal value of $|\Lambda|$. These points naturally correspond to solutions supporting a zero mode. Assuming that the number of unstable modes changes only at these points we get a relation between the number of unstable modes of the corresponding BK solutions and the branches of the W_∞ curves. Of particular interest are the curves joining $b_0 = 0$ and b_1. As was already mentioned above, these are just the curves with $W_\infty < 0$, while the $W_\infty = 0$ curve bifurcates with the 'RN' boundary for $|\Lambda| \approx 5.0646$ and those with $W_\infty > 0$ run out to $|\Lambda| = \infty$ approximating the upper resp. lower boundary for $W_\infty < 1$ resp. $W_\infty > 1$. At first sight this seems to support the hypothesis that the $W_\infty > 0$ curves have no turning points, implying the stability of these solutions. A careful numerical analysis, however, reveals that this is wrong. In fact, as Fig. 8 shows the $W_\infty = 0$ curve still has a turning point at $|\Lambda| \approx 5.104$. Thus the solutions on the upper branch of this curve between the turning point and the bifurcation point are expected to be unstable. A numerical study of the solution of the linearized equations with zero eigenvalue supports this result. Fig. 9 shows two different 'zero-energy wave-functions' δW for solutions with $W_\infty = 0$ taken below and above the dashed stability line in Fig.8. The lower one has no zero, the upper one has one, implying stability resp. existence of one negative eigenvalue corresponding to an unstable mode [24]. Neighboring curves with sufficiently small positive values of $W_\infty < 0.0005$ also have a turning point and follow the $W_\infty = 0$ curve close to the 'RN' boundary, but then turn around once more and run out to large values of $|\Lambda|$.

Our discussion shows that there is a region in the moduli space where the solutions are stable. It lies to the right of the lowest $W_\infty = 0$ curve and of the curve for the lowest zero mode and is denoted by A in Fig. 8. Then there are two regions B resp. C with solutions that have exactly one even resp. odd unstable mode, while in D they have one unstable mode of either parity. Similarly there are further regions with $2n-1$ resp. $2n$ unstable modes between the two types of curves for solutions with n nodes. All these curves terminate at the point P_∞ on the 'RN' boundary.

Acknowledgements

G.L. thanks the theory groups of Max-Planck-Institute for Physics and Max-Planck-Institute for Gravitational Physics for their kind hospitality during his visits in Munich and Golm, where part of the work was done. Work of G.L. was partly supported by INTAS grant # 00-00561 and CRDF grant # 3316.

References

[1] M.S. Volkov and D.V. Gal'tsov, *Physics Reports 319*, (1999), 1

[2] T. Torii, K. I. Maeda and T. Tachizawa, *Phys. Rev.* **D 52** (1995) 4272

[3] M.S. Volkov, N. Straumann, G.V. Lavrelashvili, M. Heusler and O. Brodbeck, *Phys. Rev.* **D 54** (1996) 7243

[4] J. Bjoraker and Y. Hosotani, *Phys. Rev. Lett.* **84** (2000) 1853

[5] R. Bartnik and J. McKinnon, *Phys. Rev. Lett.* **61** (1988) 141

[6] E. Winstanley, *Class. Quant. Grav.* **16** (1999) 1963

[7] J. Bjoraker and Y. Hosotani, *Phys. Rev.* **D 62** (2000) 043513

[8] Y. Hosotani, *J. Math. Phys.* **43** (2002) 597

[9] J.J. van der Bij and E. Radu, *Phys. Lett.* **B 536** (2002) 107

[10] E. Winstanley and O. Sarbach, *Class. Quant. Grav.* **18** (2001) 2125

[11] E. Winstanley and O. Sarbach, *Class. Quant. Grav.* **19** (2002) 689

[12] G.V. Lavrelashvili and D. Maison, *Phys. Lett.* **B 343** (1995) 214

[13] M.S. Volkov, O. Brodbeck, G.V. Lavrelashvili and N. Straumann, *Phys. Lett.* **B 349** (1995) 438

[14] N.S. Manton, *Phys. Rev.* **D 28** (1983) 2019

[15] P. Breitenlohner, P. Forgács and D. Maison, *Commun. Math. Phys.* **163** (1994) 141

[16] P. Breitenlohner, P. Forgács and D. Maison, *Nucl. Phys.* **B 442** (1995) 126

[17] P. Breitenlohner, G. Lavrelashvili and D. Maison, *Nucl. Phys.* **B 524** (1998) 427

[18] Y. Brihaye, A. Chakrabarti and D.H. Tchrakian: *J. Math. Phys.* **41** (2000) 5490

[19] G.V. Lavrelashvili, Lecture presented at International Workshop on Selected Topics of Theoretical and Modern Mathematical Physics (SIMI 96), Tbilisi, Georgia, 22-28 Sep 1996;
arXiv:gr-qc/9701049.

[20] N. Straumann Z.-H. Zhou, *Phys. Lett.* **B 237** (1990) 353

[21] O. Brodbeck, M. Heusler, G.V. Lavrelashvili, N. Straumann and M.S. Volkov, *Phys. Rev.* **D 54** (1996) 7338

[22] J. Burzlaff, *Nucl. Phys.* **B 233** (1984) 262;

[23] G. Hellwig, *Differential Operators of Mathematical Physics* Springer, Berlin (1964)

[24] I.M. Gelfand and S.V. Fomin, *Calculus of Variations* Englewood Cliffs N.J., Prentice Hall (1963)

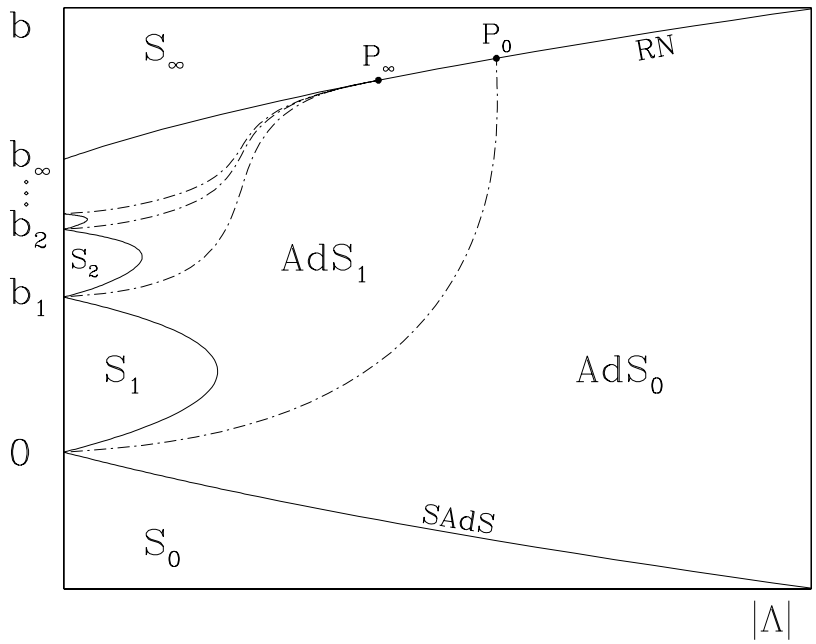

Figure 1: Schematic plot of the moduli space: the solid lines are the boundary of AdS; the dashed-dotted lines are curves $W_\infty = 0$.

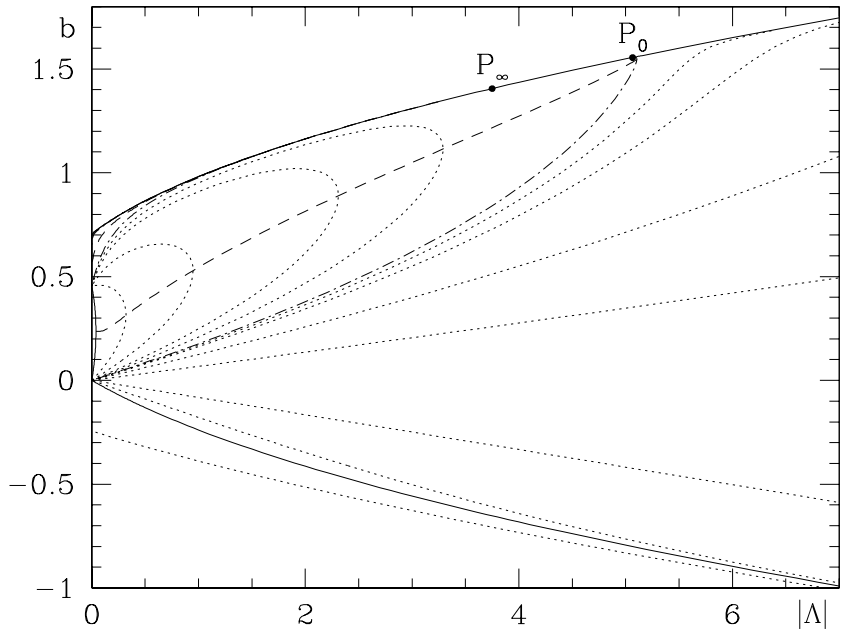

Figure 2: The numerically determined moduli space: solid and dashed-dotted lines as in Fig. 1, zero-mode curves are dashed, curves for several W_∞ resp. W_0 =const. are dotted.

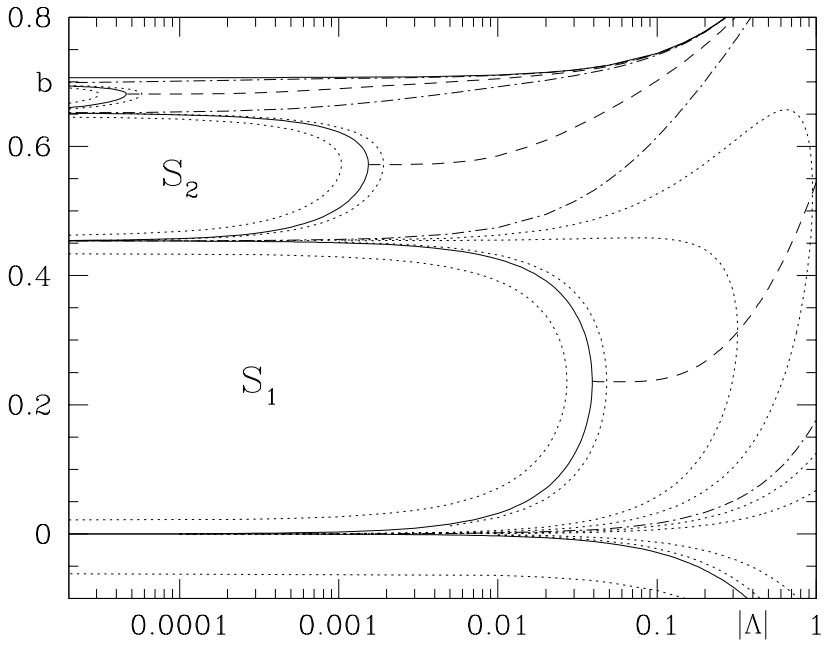

Figure 3: Small Λ part of Fig. 2 with a logarithmic scale.

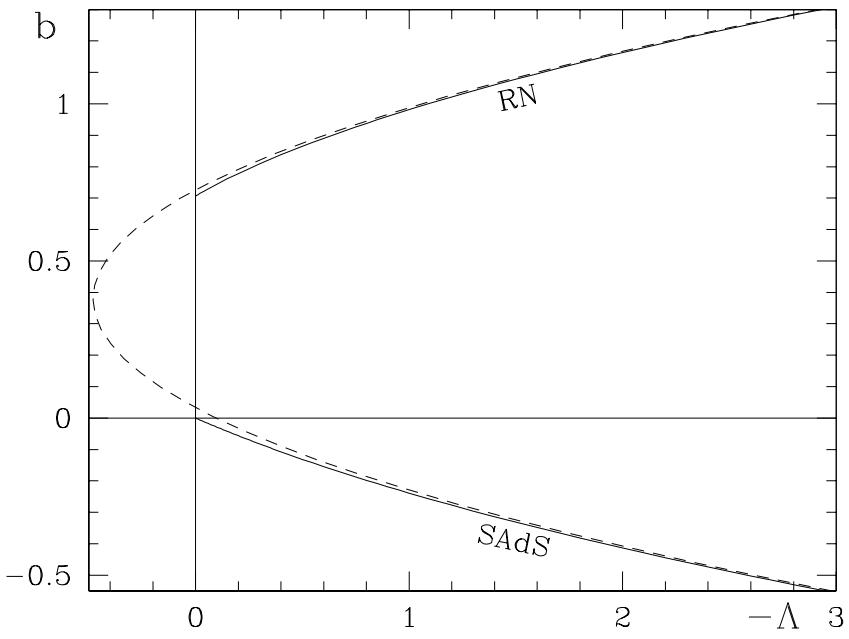

Figure 4: The parabola fit for large $|\Lambda|$ to the boundary curves of AdS.

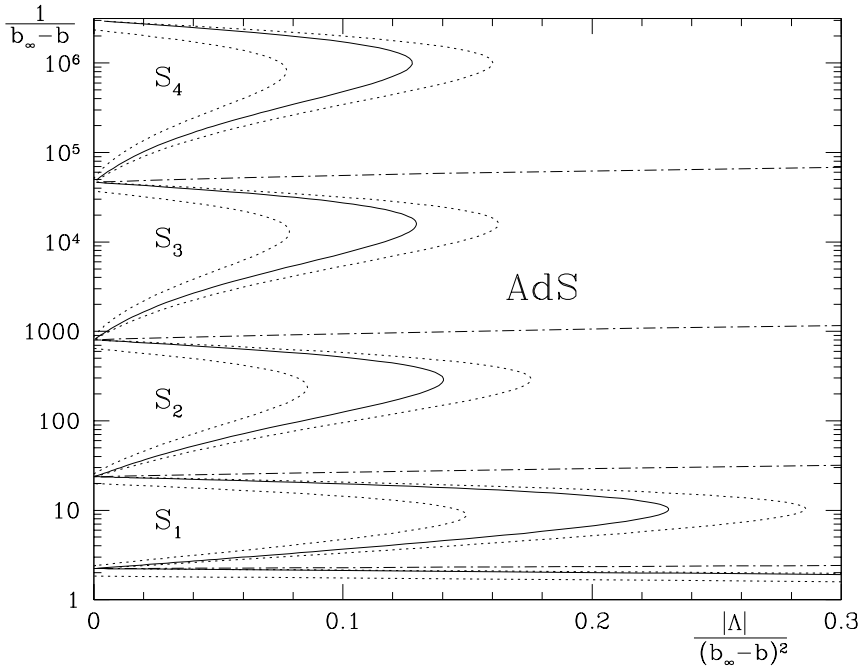

Figure 5: The rescaled regions S_n: the dashed-dotted lines are curves $W_\infty = 0$, the dotted lines in AdS are curves for $|W_\infty| = 10$, those in $S_0, \ldots, S_4$ are curves for $|W_0| = 6.5$, 40, 245, 1505, and 9231.

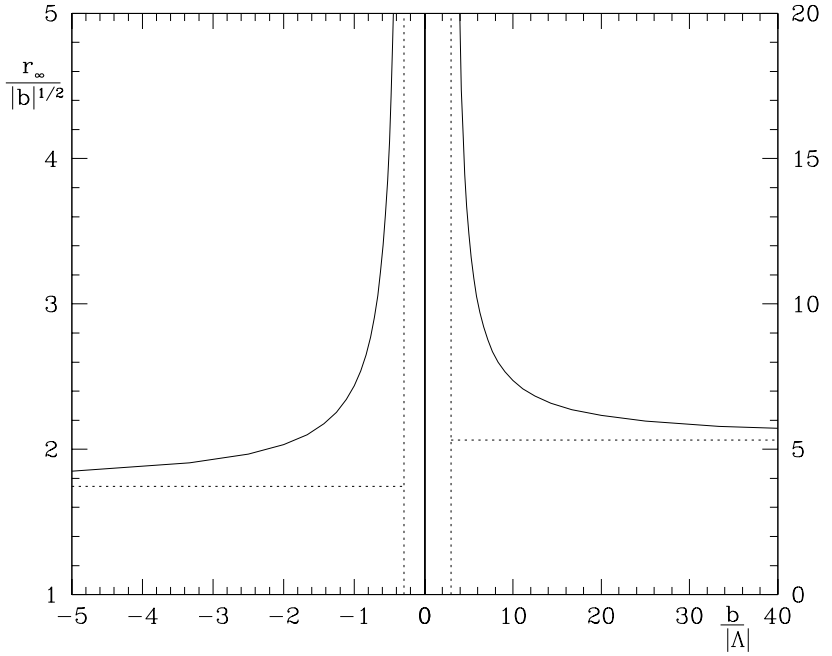

Figure 6: The radius r_∞ for singular solutions in the AdS background as a function of $\bar{b} = \frac{b}{|\Lambda|}$; the vertical dotted lines at $\bar{b} = -0.294582$ and 2.970497 represent the boundary for singular solutions, the horizontal dotted lines are the BK values $\bar{r} = 1.74575$ and 5.31661 for $\Lambda = 0$.

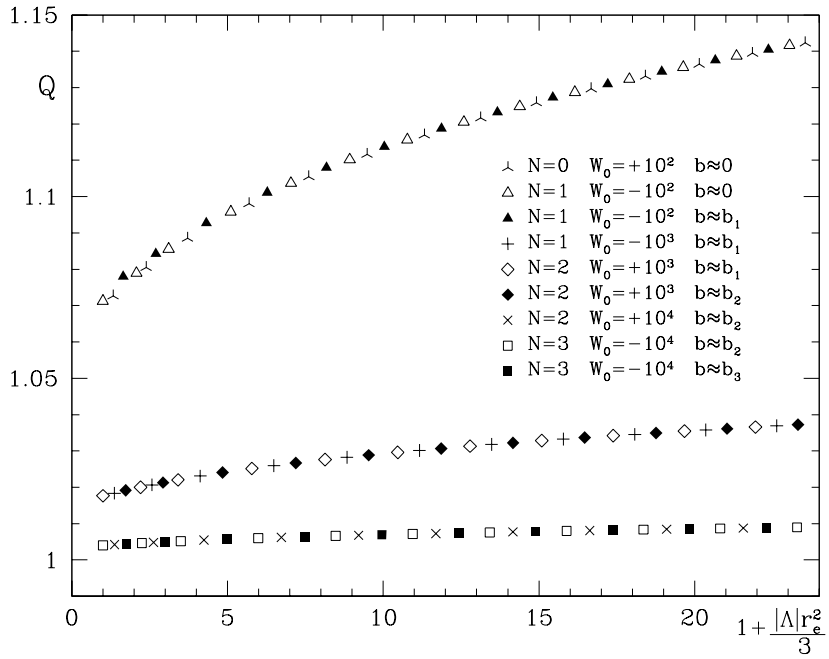

Figure 7: A plot of the quotient Q of th l.h.s. and r.h.s. of Eq. (31) for solutions with $N = 0, \ldots, 3$ nodes and various values of W_0.

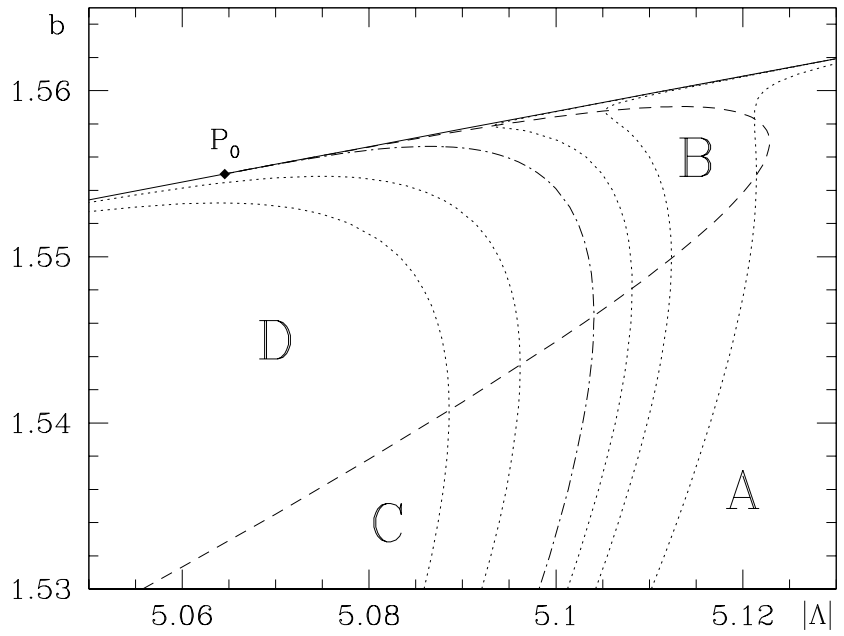

Figure 8: Enlarged view of the moduli space near P_0 with W_∞ curves in the range $\pm 4 \cdot 10^{-4}$; the regions A, ..., D with different numbers of even and odd unstable modes are separated by the dashed-dotted W_∞ curve and the dashed zero-mode curve.

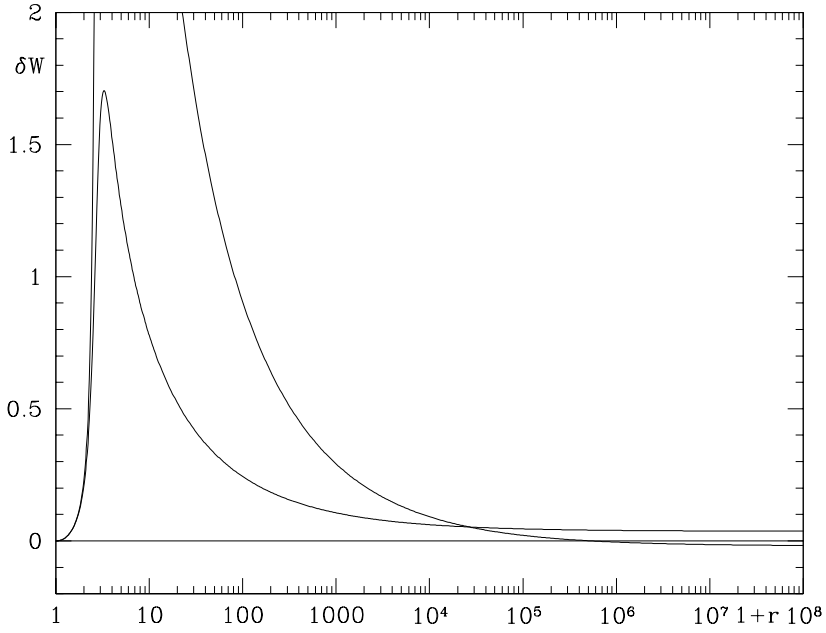

Figure 9: Zero energy wave functions δW for nodeless solutions with $W_\infty = 0$ for $b = 1.5$, $\Lambda = -5.075439$ lying below and $b = 1.553$, $\Lambda = -5.101469$ lying above the zero-mode curve.